

Wave Scattering by Superluminal Space-Time Modulated Slabs and Symmetries with the Subluminal Case

Zoé-Lise Deck-Léger and Christophe Caloz*

Dpt. of Electrical Engineering, Polytechnique Montréal, Montréal, QC H3T 1J4, Canada

The paper solves the problem of electromagnetic wave scattering from a superluminal space-time modulated (STM) slab and reveals fundamental symmetries with respect to the case of a subluminal STM slab in terms of scattering amplitudes and angles. Specifically, we show that the amplitude and angle of the reflected wave for the superluminal case are symmetric to those of the subluminal case for inverse velocities. This work may serve as a theoretical foundation for emerging STM metamaterials.

Space-time (ST) media are media whose constitutive parameters vary in space and time. They may be realized using either *matter* motion or *wave* motion. The former are generally referred to as “moving media” while the latter may be referred to as “ST-modulated (STM) media”. Moving and STM media both produce frequency shifting and amplification, but also exhibit fundamental differences. Moving media involve drag, as theoretically predicted by Fresnel [1] and experimentally demonstrated by Fizeau [2], and are therefore generally seen as bianisotropic by an observer at rest, as shown by Minkowski [3]. In contrast, STM media involve no drag and the structure of their constitutive parameters is therefore identical to that of the corresponding motionless medium.

Moving media are restricted to subluminal velocities, since no object can travel faster than the speed of light, and related experiments are cumbersome or impractical, especially in the relativistic regime. On the other hand, STM media may be superluminal, and even reach infinite velocity. Moreover, they may be experimentally realized in transversally-perturbed systems, such as acoustic structures [4], ferrite-loaded waveguides [5], transmission lines [6], plasmas [7], and emerging metamaterial technologies will likely offer a host of new related opportunities in this area. Therefore, STM media may offer a broader range of functionalities and present greater perspectives towards applications. For these reasons, we focus here on STM medium, and we specifically study the scattering of electromagnetic waves in such a medium.

The ST modulation may concern any of the bianisotropic medium parameters, $\chi(\mathbf{r}, t)$, (permittivity, permeability, electro-magnetic and magneto-electric coupling parameters) and may assume various profiles, such as step, rectangular, periodic, aperiodic and random profiles. The most fundamental profile is the STM Heaviside step discontinuity, $\chi(\mathbf{r}, t) = H(\mathbf{r} - v_s t)$, which corresponds to a single interface between two different media. Richer physics occur in the case of an STM slab, $\chi(\mathbf{r}, t) = \text{rect}(\mathbf{r} - v_s t)$, corresponding to the succession of two STM interfaces. We investigate here the scattering of waves in superluminal STM slabs and find fundamental symmetries with respect to the subluminal case in terms

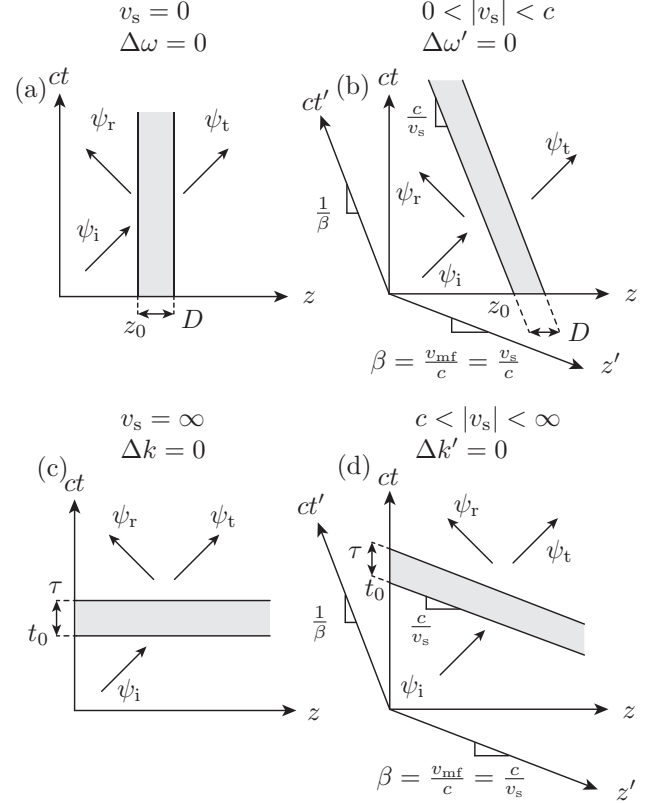


FIG. 1. Classification of space-time modulated (STM) slabs in terms of their velocity, v_s , relative to the velocity of light c . (a) Spatial slab. (b) Subluminal STM (approaching) slab. (c) Temporal slab. (d) Superluminal STM, or “time-space”, (approaching) slab. The unprimed and primed axes correspond to the static and moving frames, respectively.

of scattering amplitudes and angles.

STM slabs may be classified according to their velocity, v_s , using Minkowski diagrams [8], as shown in Fig. 1 for the case of discontinuity in the z -direction. In these diagrams, ψ_i , ψ_r and ψ_t represent the incident, reflected and transmitted waves, respectively, while the associated arrows represent the corresponding world lines or trajectories.

A *spatial* slab is a non-moving ($v_s = 0$, static) slab,

$\chi(z, t) = \text{rect}\{[z - (z_0 + D/2)]/D\} \neq \chi(t)$, corresponding to a strip parallel to the ct axis, as shown in Fig. 1(a). In such a system, the wave experiences no temporal frequency change, i.e. $\Delta\omega = 0$. A *subluminal* STM slab, $\chi(z, t) = \text{rect}\{[z - (z_0 + D/2) - v_s t]/D\}$ with $0 < |v_s| < c$, corresponds to an oblique version of this strip with slope (c/v_s) greater than 1, as shown in Fig. 1(b). Such a slab appears static in the frame moving with velocity $v_{\text{mf}} = v_s$, so that $\Delta\omega' = 0$, and is parallel to the ct' axis, whose slope is $c/v_{\text{mf}} = 1/\beta$, i.e. $\beta = v_s/c$.

The dual system of the spatial slab is the *temporal* slab, an instantaneous variation ($v_s = \infty$) of the medium properties everywhere in space, $\chi(z, t) = \text{rect}\{[t - (t_0 + \tau/2)]/\tau\} \neq \chi(z)$, corresponding to a strip parallel to the z axis, as shown in Fig. 1(c). In this case, the temporal frequencies change but the spatial frequencies are conserved, i.e. $\Delta\mathbf{k} = 0$. Finally, the dual of the subluminal slab is the *superluminal* slab, $\chi(z, t) = \text{rect}\{[t - (t_0 + \tau/2) - z/v_s]/\tau\}$ with $\infty > |v_s| > c$, corresponding to an oblique version of this strip, with slope (c/v_s) smaller than 1, as shown in Fig. 1(d). Such a slab appears purely temporal in the moving frame, so that $\Delta\mathbf{k}' = 0$, and is parallel to the z' axis, i.e. $\beta = c/v_s$. Note that this problem *could not* be solved in a frame where the slab appears at rest, as done in the subluminal case, since this would lead to $\beta > 1$, and hence to complex quantities in the Lorentz transformation! Also note that whereas a subluminal STM (or purely spatial) interface supports a reflected wave propagating in the first medium, the superluminal STM (or purely temporal) interface rather supports a backward wave propagating in the final medium, since the interface moves faster than this wave. The superluminal slab is the system of primary interest in this work, since it has not been described anywhere else.

The literature contains a number of reports on STM media. Several authors have studied wave scattering by subluminal half-spaces [6, 9] and slabs [10, 11] [Fig. 1(b)]. Scattering of scalar waves by temporal discontinuities [Fig. 1(c)] has been investigated in [7, 12, 13]. Reports on superluminal discontinuities [Fig. 1(d)] are scarcer, but corresponding frequency transformations for normal incidence have been discussed in [14], and frequency-amplitude transformations, also restricted to normal incidence, have been computed in [15].

The fields before, during (or inside) and after the superluminal slab [Fig. 1(d)], assuming wave propagation in the xz -plane and y -polarization, may be written as

$$\mathbf{E}_m^\pm = A_m^\pm e^{i(k_{xm}^\pm x + k_{zm}^\pm z \mp \omega_m^\pm t)} \hat{\mathbf{y}}, \quad (1a)$$

where the subscript m denotes the medium ($m = 1, 2, 3$) and the superscripts $+$ and $-$ indicate forward and backward propagation, respectively. The corresponding trajectories are drawn in Fig. 2. Inserting (1a) into Maxwell-

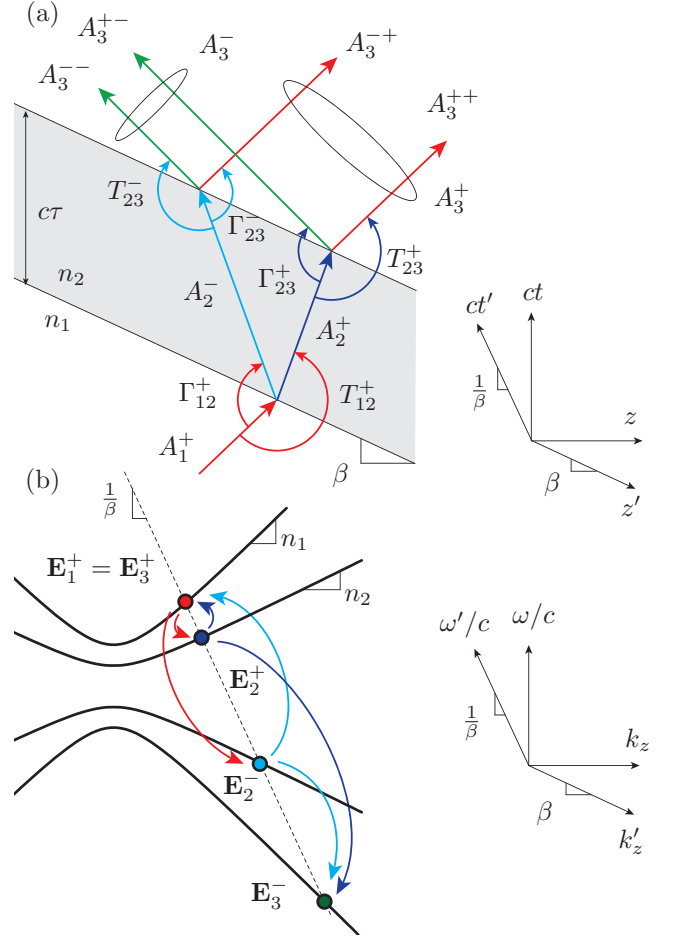


FIG. 2. Scattering from a superluminal STM slab. (a) Wave trajectories in the Minkowski diagram, leading to (4) and (5). (b) Corresponding frequencies in the dispersion diagram, leading to (6) and (7). The ST axes for moving and stationary frames in direct and inverse space are drawn on the right.

Faraday equation yields

$$\mathbf{B}_m^\pm = \mp A_m^\pm \frac{n_m}{c} e^{i(k_{xm}^\pm x + k_{zm}^\pm z \mp \omega_m^\pm t)} (\cos \theta_m^\pm \hat{\mathbf{x}} - \sin \theta_m^\pm \hat{\mathbf{z}}), \quad (1b)$$

where n_m is the refractive index of medium m , $k_{zm}^\pm = k_m^\pm \cos \theta_m^\pm$ and $k_{xm}^\pm = k_m^\pm \sin \theta_m^\pm$ with $k_m^\pm = \omega_m^\pm n_m/c$ are the wavenumbers in medium m and θ_m^\pm is the propagation angle defined from the normal to the interface. Assuming that the media are monoisotropic, dispersionless, linear, and homogeneous, the constitutive relations in each region read

$$\mathbf{D}_m^\pm = \epsilon_m \mathbf{E}_m^\pm, \quad \mathbf{B}_m^\pm = \mu_m \mathbf{H}_m^\pm, \quad (1c)$$

with permittivity ϵ_m and permeability μ_m .

Since at a temporal interface continuity regards the \mathbf{D} and \mathbf{B} fields [12, 16], at a superluminal STM interface it concerns the same fields in the moving frame, i.e.

$$[\mathbf{D}'_m = \mathbf{D}'_{m+1}]_{t'=0}, \quad [\mathbf{D}'_m = \mathbf{D}'_{m+1}]_{t'=0}. \quad (2)$$

In order to solve (2), one must express the fields (1) in the moving frame, namely, using Lorentz transformation [17],

$$c\mathbf{D}'_{\perp} = \gamma(c\mathbf{D}_{\perp} + \boldsymbol{\beta} \times \mathbf{H}_{\perp}), \quad c\mathbf{B}'_{\perp} = \gamma(c\mathbf{B}_{\perp} - \boldsymbol{\beta} \times \mathbf{E}_{\perp}), \quad (3)$$

where $\gamma = 1/\sqrt{1-\beta^2}$, with β previously defined as $\beta = v_{mf}/c = c/v_s$ [see Fig. 1(d)]. Equation (3) represents the field components that are perpendicular to the direction of the modulation, while the parallel components are unchanged. Inserting (3) into (2) and substituting (1) in the resulting equations yields, with the help of Fig. 2(a), the superluminal STM Fresnel coefficients at the interface between media m and $m+1$ for the forward incident wave

$$T_{m,m+1}^+ = \frac{A_{m+1}^{++}}{A_m^+} = \frac{f_m^+}{f_{m+1}^+} \frac{\eta_{m+1}^2 Z_m^+ + \eta_m^2 Z_{m+1}^-}{\eta_m^2 (Z_{m+1}^- + Z_{m+1}^+)}, \quad (4a)$$

$$\Gamma_{m,m+1}^+ = \frac{A_{m+1}^{+-}}{A_m^+} = \frac{f_m^+}{f_{m+1}^-} \frac{\eta_{m+1}^2 Z_m^+ - \eta_m^2 Z_{m+1}^+}{\eta_m^2 (Z_{m+1}^- + Z_{m+1}^+)}, \quad (4b)$$

where $Z_m^{\pm} = \eta_m g_m^{\pm}/f_m^{\pm}$, $g_m^{\pm} = n_m \mp \beta \cos \theta_m^{\pm}$ and $f_m^{\pm} = n_m \cos \theta_m^{\pm} \mp \beta$, with η_m being the intrinsic impedance of medium m . The coefficients for the backward incident wave exactly correspond to those for the forward incident wave with changed velocity sign, since scattering of a backward wave on a receding discontinuity is strictly equivalent to scattering of a forward wave on an approaching discontinuity. Thus, $T_{m,m+1}^- = T_{m,m+1}^+(-v_s)$, $\Gamma_{m,m+1}^- = \Gamma_{m,m+1}^+(-v_s)$. Note that the results in (4) reduce to those presented in [15] in the particular case normal incidence ($\theta_1^+ = 0$).

Whereas the subluminal STM (or purely spatial) slab supports an infinite number of waves scattered by the two interfaces, due to spatial reflection, the superluminal (or purely temporal) slab scatters only two waves, a forward one and a backward one, at each interface, leading to a total of four scattered waves at the output of the system, as seen in Fig. 2(a). The corresponding overall STM slab scattering coefficients are obtained with the help of Fig. 2(a) by multiplying the successive scattering events and adding the final co-directed contributions, which yields

$$T = \frac{A_3^+}{A_1^+} = T_{12}^+ T_{23}^+ e^{-i\tau\omega_2^+} + \Gamma_{12}^+ \Gamma_{23}^- e^{i\tau\omega_2^-}, \quad (5a)$$

$$\Gamma = \frac{A_3^-}{A_1^+} = T_{12}^+ \Gamma_{23}^+ e^{-i\tau\omega_2^+} + \Gamma_{12}^+ T_{23}^- e^{i\tau\omega_2^-}, \quad (5b)$$

where the terms $e^{\mp i\tau\omega_2^{\pm}}$ correspond to the phase accumulated across the slab.

We shall now derive the scattered ST frequencies $(\mathbf{k}_m^{\pm}, \omega_m^{\pm})$. These quantities are first diagrammatically

localized in the dispersion diagram in Fig. 2(b), and will be later derived mathematically. The diagram is constructed as follows: 1) Draw the frequency axes of both the static and moving frames; 2) Plot the dispersion curves of media 1 \equiv 3 and 2 for a fixed k_x , corresponding to the incidence angle $\theta_1^+ = \sin^{-1}(k_{x1}^+/k_1^+)$; 3) Locate the incident field \mathbf{E}_1^+ ; 4) Locate the scattered field frequencies at the intersections of the dispersion curves and the straight line parallel to ω' corresponding to conserved k'_z .

Wavenumber conservation in the moving frame, $\Delta \mathbf{k}' = 0$, is expressed in the rest frame, using Lorentz transformation, as

$$k_{1z}^+ - \beta \frac{\omega_1^+}{c} = k_{2z}^{\pm} \mp \beta \frac{\omega_2^{\pm}}{c} = k_{3z}^{\pm} \mp \beta \frac{\omega_3^{\pm}}{c}, \quad (6a)$$

$$k_{1x}^+ = k_{2x}^{\pm} = k_{3x}^{\pm}. \quad (6b)$$

The scattered temporal frequencies are subsequently found by substituting $k_{mz}^{\pm} = k_m^{\pm} \cos \theta_m^{\pm}$ and $k_{mx}^{\pm} = k_m^{\pm} \sin \theta_m^{\pm}$ with $k_m^{\pm} = \omega_m^{\pm} n_m/c$ into (6a). The results are

$$\omega_2^{\pm} = \omega_1^+ \frac{n_1 \cos \theta_1^+ - \beta}{n_2 \cos \theta_2^{\pm} \mp \beta} = \omega_1^+ \frac{f_1^+}{f_2^{\pm}}, \quad (7a)$$

$$\omega_3^+ = \omega_1^+ \frac{f_1^+}{f_3^+} = \omega_1^+, \quad \omega_3^- = \omega_1^+ \frac{f_1^+}{f_3^-}. \quad (7b)$$

The scattered spatial frequencies, or scattering angles, are obtained by performing the same substitutions into (6b) and (6a), and dividing the resulting equations, which yields

$$\frac{\sin \theta_1^+}{\cos \theta_1^+ - \beta/n_1} = \frac{\sin \theta_2^{\pm}}{\cos \theta_2^{\pm} \mp \beta/n_2} = \frac{\sin \theta_3^{\pm}}{\cos \theta_3^{\pm} \mp \beta/n_1}. \quad (8)$$

The angles of the scattered waves in the third medium are explicitly found after algebraically manipulating (8), closely following [9], as detailed in [18]

$$\cos \theta_3^+ = \cos \theta_1^+, \quad \cos \theta_3^- = \frac{\cos \theta_1^+ (1 + \beta^2) - 2\beta}{1 + \beta^2 - 2\beta \cos \theta_1^+}. \quad (9)$$

Equations (9) and (7b) reveal that the wave forwardly transmitted across the slab has the same angle and frequency as the incident wave, while the backwardly transmitted wave depends on β , in accordance with the diagrammatic construction in Fig. 2(b).

Interesting observations may be done in the particular case of normal incidence, where $\theta_1^+ = 0$ and therefore also $\theta_2^+ = \theta_2^- = 0$, according to (8). Equation (7a) yields then $\omega_2^{\pm} = \omega_1^+ (n_1 - \beta)/(n_2 \mp \beta)$, which expectedly reduces to $\omega_2^{\pm} = \omega_1^+ (n_1/n_2)$ in the limiting case of the purely temporal slab ($\beta = c/v_s \rightarrow 0$) [12]. Moreover, inserting the second equality of (7a) into (4) yields $T_{m,m+1}^+ \propto \omega_2^+/ \omega_1^+$, $\Gamma_{m,m+1}^+ \propto \omega_2^- / \omega_1^+$, indicating that

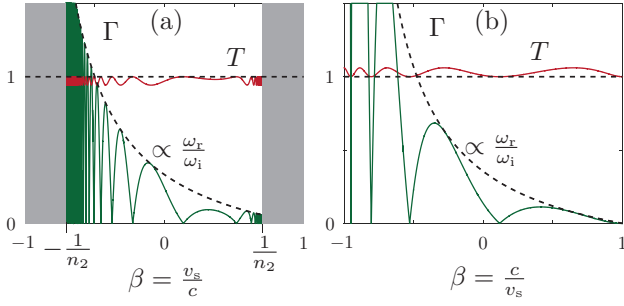


FIG. 3. Scattering coefficients versus β for a wave with frequency $\omega_1^+ = 1$ rad/s normally ($\theta_1^+ = 0$) incident on a slab with index $n_2 = \sqrt{2}$ surrounded by media of indices $n_1 = n_3 = 1$. (a) Subluminal STM slab with spatial extent $D = 5$ m. The grey areas correspond to regions without analytical solutions [15]. (b) Superluminal STM slab with duration $\tau = 5$ s, computed by (5). Note the inverted parameter β from (a) to (b), corresponding to the symmetry (10).

the scattering coefficients are proportional to the ratio of scattered versus incident frequencies. Equations (5) then yield $T \propto \omega_3^+/\omega_1^+ = 1$ and $\Gamma \propto \omega_3^-/\omega_1^+$, a result that also holds for subluminal STM slabs [6, 10]. Figure 3 compares the $T(\beta)$ and $\Gamma(\beta)$ functions for the subluminal [Fig. 3(a)] and superluminal [Fig. 3(b)] cases, which shows the fundamental symmetry

$$\text{envelope} \{ \Gamma_{v_s > c}(v_s) \} \propto \text{envelope} \{ \Gamma_{v_s < c}(1/v_s) \}, \quad (10a)$$

and also shows the result

$$\min(T_{v_s > c}) = \max(T_{v_s < c}) = 1 \neq f(v_s). \quad (10b)$$

Another fundamental symmetry is found when comparing the scattered angles. Indeed, the angle of the wave, $\theta_3^-(v_s)$, given by (9), is related to the angle of the wave reflected by a subluminal STM slab, described in [9], according to the relation

$$\theta_{3^-}^-(v_s > c) = \theta_{3^-}^-(v_s < c)(1/v_s). \quad (11)$$

Figure 4 illustrates this symmetry. The top diagram is constructed as in Fig. 2(b) for the four cases in Fig. 1. The dispersion curve for the second medium is not drawn here since we are interested only in the waves at the output of the slab. The isofrequency diagram at the bottom of the figure is constructed as follows: 1) Project the k_z value onto this (k_x, k_z) diagram; 2) Locate the intersection with the constant k_x line; 3) Draw the isofrequency circles with radii corresponding the intersection points; 4) Draw the normal to these isofrequency curves to find the corresponding group velocities ($\mathbf{v}_g = \nabla_{\mathbf{k}}\omega$). We shall next specifically describe the four slab systems.

The case of the *spatial* slab [Fig. 1(a)] is solved by drawing the horizontal dashed line corresponding to conserved temporal frequency from the incident wave point

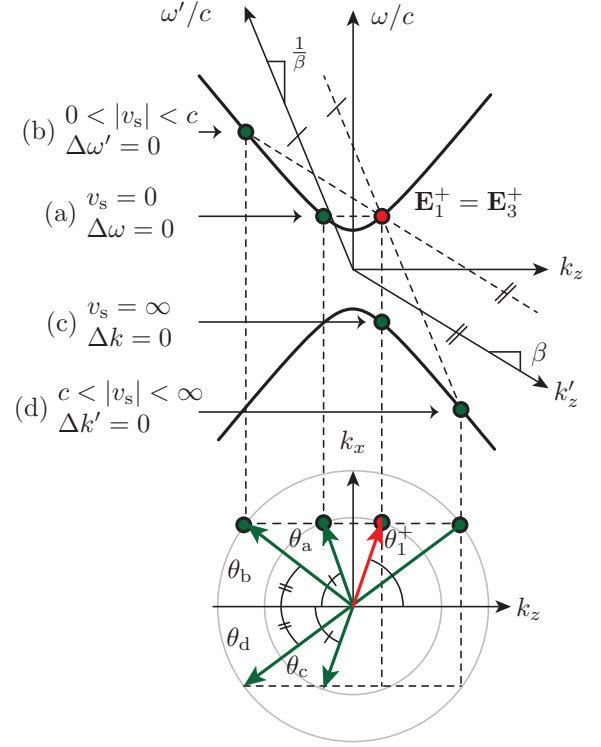


FIG. 4. Derivation the ST frequencies scattered by the STM slab under oblique incidence using dispersion and isofrequency diagrams for the four classes of STM slabs in Fig. 1. Note the symmetry between the subluminal and superluminal angles, corresponding to the result (11).

at the top of Fig. 4. The subsequent projection onto the isofrequency diagram shows the direction of the scattered wave which corresponds, as expected, to specular reflection. The case of the *subluminal* slab [Fig. 1(b)] is solved, remembering that the temporal frequencies in the moving frame (ω') are conserved, by drawing the dashed line parallel to the k'_z axis, and projecting the result onto the isofrequency diagram. This shows that the scattered angle is smaller than for the spatial case. In the case of the *temporal* slab [Fig. 1(c)], the conserved frequencies are the spatial ones, and the temporal frequency is negative. Therefore, the reflected wave is collinear but opposite to the incident wave. Finally, for the *superluminal* ($v_s > c$) slab [Fig. 1(d)], the frequency is also negative, with the same magnitude as that of the subluminal one, and the scattered angle is symmetric to the subluminal one.

We have solved the problem of electromagnetic wave scattering from a superluminal slab. We mathematically and diagrammatically found fundamental symmetries between the subluminal and superluminal cases. The discovery of these symmetries both opens new fundamental questions in physics and forms a theoretical foundation for novel STM media.

* Email: see <http://www.calozgroup.org>

- [1] A. J. Fresnel, "Lettre d'Augustin Fresnel à François Arago sur l'influence du mouvement terrestre dans quelques phénomènes d'optique," *Ann. Chim. Phys.* **9**, 57–66 (1818).
- [2] H. Fizeau, "Sur les hypothèses relatives à l'éther lumineux, et sur une expérience qui paraît démontrer que le mouvement des corps change la vitesse avec laquelle la lumière se propage dans leur intérieur," *C.R. Acad. Sci.* **33**, 349 (1851).
- [3] H. Minkowski, "Die Grundgleichungen für die elektromagnetischen Vorgänge in bewegten Körper," *Nachr. Ges. Wiss. Göttingen*, 53–111 (1908).
- [4] M. B. Zanjani, A. R. Davoyan, A. M. Mahmoud, N. Engheta, and J. R. Lukes, "One-way phonon isolation in acoustic waveguides," *Appl. Phys. Lett.* **104**, 081905 (2014).
- [5] D. Holberg and K. Kunz, "Parametric properties of fields in a slab of time-varying permittivity," *IEEE Trans. Antennas. Propag.* **14**, 183–194 (1966).
- [6] J. R. Pierce, "Use of the principles of conservation of energy and momentum in connection with the operation of wave-type parametric amplifiers," *J. Appl. Phys.* **30**, 1341–1346 (1958).
- [7] D. K. Kalluri, *Electromagnetics of Time Varying Complex Media: Frequency and Polarization Transformer* (CRC Press, 2010).
- [8] H. Minkowski, "Raum und Zeit," *Jahresbericht der Deutschen Mathematiker-Vereinigung* **18**, 75–88 (1909).
- [9] K. Kunz, "Plane electromagnetic waves in moving media and reflections from moving interfaces," *J. Appl. Phys.* **51**, 873–884 (1980).
- [10] C. Yeh and K. F. Casey, "Reflection and transmission of electromagnetic waves by a moving dielectric slab," *Phys. Rev.* **144**, 665–669 (1966).
- [11] C. S. Tsai and B. A. Auld, "Wave interactions with moving boundaries," *J. Appl. Phys.* **38**, 2106–2115 (1967).
- [12] F. R. Morgenthaler, "Velocity modulation of electromagnetic waves," *IEEE Trans. Microw. Theory Techn.* **6**, 167–172 (1958).
- [13] L. Felsen and G. M. Whitman, "Wave propagation in time-varying media," *IEEE Trans. Antennas. Propag.* **18**, 242–253 (1970).
- [14] M. Lampe, E. Ott, and J. Walker, "Interaction of electromagnetic waves with a moving ionization front," *Phys. Fluids* **21**, 42–54 (1978).
- [15] F. Biancalana, A. Amann, A. V. Uskov, and E. P. O'Reilly, "Dynamics of light propagation in spatiotemporal dielectric structures," *Phys. Rev. E* **75**, 046607 (2007), equation 32.
- [16] J. R. Zurita-Sánchez, P. Halevi, and J. C. Cervantes-González, "Reflection and transmission of a wave incident on a slab with a time-periodic dielectric function $\epsilon(t)$," *Phys. Rev. A* **79**, 053821 (2009).
- [17] E. J. Rothwell and M. J. Cloud, *Electromagnetics, Second Edition* (CRC Press, 2009).
- [18] "See supplementary material at [] for the complete derivation of (9)," .